AD-A166 242 EXPERIMENTAL STUDY OF ELECTRONIC STATES AT METAL-DIELECTRIC INTERFACES(U) CORNELL UNIV ITHACA NY A J SIEVERS 23 DEC 85 AFOSR-TR-86-0077 AFOSR-81-0121 1/1

UNCLASSIFIED F/G 7/4 NL

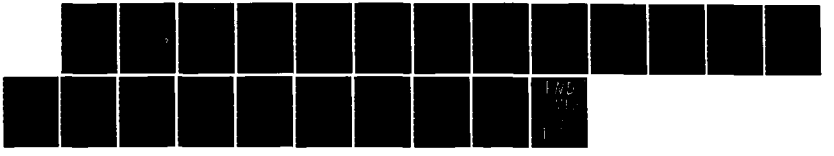

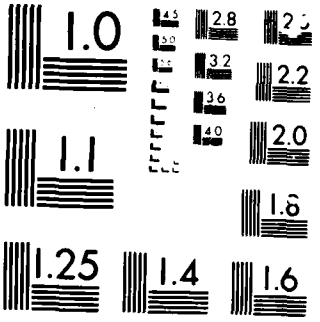

(2)

Interim Technical Report

February 2, 1981 - February 1, 1982

Experimental Study of Electronic States at METAL-DIELECTRIC Interfaces

Submitted to: AFOSR/NE
Att: Capt. G. T. Rosalia

Submitted by: Cornell University
Ithaca, NY 14853

Principal Investigator: A. J. Sievers
Prof. of Physics
Lab. of Atomic and
Solid State Physics

UNCLASSIFIED

SECURITY CLASSIFICATION OF THIS PAGE

AD-A166 242

(2)

REPORT DOCUMENTATION PAGE

1a. REPORT SECURITY CLASSIFICATION: UNCLASSIFIED	1b. RESTRICTIVE MARKINGS:
2a. SECURITY CLASSIFICATION AUTHORITY: open	3. DISTRIBUTION/AVAILABILITY OF REPORT: Approved for public release; distribution unlimited.
2b. DECLASSIFICATION/DOWNGRADING SCHEDULE:	
4. PERFORMING ORGANIZATION REPORT NUMBER(S):	5. MONITORING ORGANIZATION REPORT NUMBER(S): AFOSR-TR- 86-0077
6a. NAME OF PERFORMING ORGANIZATION: Cornell University; 6b. OFFICE SYMBOL (If applicable):	7a. NAME OF MONITORING ORGANIZATION: AFOSR
6c. ADDRESS (City, State and ZIP Code): Clark Hall, Cornell University, Ithaca, NY 14850-2501	7b. ADDRESS (City, State and ZIP Code): Bolling AFB, Bldg. 410, Washington, D.C. 20332
8a. NAME OF FUNDING/SPONSORING ORGANIZATION: AFOSR; 8b. OFFICE SYMBOL (If applicable): NE	9. PROCUREMENT INSTRUMENT IDENTIFICATION NUMBER: AFOSR-81-0121
8c. ADDRESS (City, State and ZIP Code): Bolling AFB, Bldg. 410, Washington, D.C. 20332	10. SOURCE OF FUNDING NOS. — PROGRAM ELEMENT NO.: 61102F; PROJECT NO.: 2306; TASK NO.: B2; WORK UNIT NO.:
11. TITLE (Include Security Classification): Experimental Study of Electronic States at Metal-Dielectric Interfaces	
12. PERSONAL AUTHOR(S): A. J. Sievers	
13a. TYPE OF REPORT: Interim Technical; 13b. TIME COVERED: FROM 2/2/81 TO 2/1/82	14. DATE OF REPORT (Yr., Mo., Day): 12/23/85; 15. PAGE COUNT: 19
16. SUPPLEMENTARY NOTATION:	
17. COSATI CODES — FIELD: ; GROUP: ; SUB. GR.:	18. SUBJECT TERMS (Continue on reverse if necessary and identify by block number): Infrared, electromagnetic, SEW's

19. ABSTRACT (Continue on reverse if necessary and identify by block number)

Far infrared surface electromagnetic wave (SEW) propagation lengths have been measured for Ge coated Au and Pb surfaces. Their values are in reasonable agreement with Drude theory. An edge coupler is used to transmit 84 cm^{-1} SEW's across 1.5 to 7.5 cm pathlengths on optically thick metal film surfaces with Ge overlayers ranging in thickness from one to two microns. We are unable to couple to far infrared SEW's on bare metal surfaces because their fields extend so far off the surface; however, for coated surfaces the SEW is much more confined and coupling does occur. Bare metal SEW propagation lengths of 150 cm for Au, and 35 cm for Pb are inferred from our measurements, in reasonable agreement with our metal film d.c. resistivities. Anomalously short SEW propagation lengths reported by previous investigators are reinterpreted in terms of bulk wave packet spreading.

20. DISTRIBUTION/AVAILABILITY OF ABSTRACT: UNCLASSIFIED/UNLIMITED ☒ SAME AS RPT ☐ DTIC USERS ☐	21. ABSTRACT SECURITY CLASSIFICATION: UNCLASSIFIED
22a. NAME OF RESPONSIBLE INDIVIDUAL: ~~A. J. Sievers~~ Capt Kevin Wall	22b. TELEPHONE NUMBER (Include Area Code): ~~(607) 256-6422~~ 767-4931; 22c. OFFICE SYMBOL: NE

DD FORM 1473, 83 APR — EDITION OF 1 JAN 73 IS OBSOLETE.

UNCLASSIFIED

I ABSTRACT

By means of new infrared techniques we are exploring both the time and frequency domain spectra of electronic interface states. These data can be used to obtain information specific to interfaces such as mobility and diffusion, lifetimes, energy levels and the density of states.

II PROJECT OBJECTIVES

We shall continue the development of new infrared techniques which are ideally matched to the interface problem and then use these techniques to measure and characterize the physical properties of electronic states at metal-dielectric interfaces. Since these techniques rely on evanescent electromagnetic waves a closely related objective is to explore the near field electrodynamics of structures which produce evanescent fields. Metal semiconductor interfaces can be studied with broadband SEW spectroscopy using incoherent thermal radiation for a source and the surface photoconductivity for a detector. With coherent sources power dependent absorption measurements and also light scattering from surface electrokinetic phenomena become feasible. These instruments will not only be used to probe the excitation spectra of metal-semiconductor interface states but also to explore the magnetic field dependence of the energy levels in n-type InSb-NiSb eutectic. From past experience with donors in bulk InSb, we can anticipate that IR techniques coupled with external perturbations such as temperature and d.c. electric field will provide a large amount of detailed spectroscopic information about the dynamical behavior of carriers in this submicron composite structure.

III ACCOMPLISHMENTS

A. Broadband Surface Plasmon Spectroscopy

Infrared surface electromagnetic wave are bound TM modes that exist at metal surfaces.[1] They propagate along the surface with a phase velocity less than, but close to, the speed of light and have field amplitudes which are maximal at the surface and decay exponentially with distance away from it. On good conductors, infrared SEW's propagate for distances many times their wavelength and can be used to probe the optical properties of surface.[2,3] In previously reported work, SEW's excited at a single frequency or several discrete frequencies by coherent radiation from infrared lasers have been used to study bare metal surfaces,[4-7] metal surfaces with thin overlayers[7-10] and molecules adsorbed on metal surfaces.[9-11] In the past spectroscopic studies with thermal sources have not been possible with the SEW transmission technique because of insufficient energy throughput.

The first study of the propagation of surface plasmons excited by an incoherent source is reported in publication (A). Four different types of dielectric-metal edge couplers were fabricated for this work. A schematic representation of each coupler is shown in Figure 1. The original prism coupler[10] is shown in Figure 1(a). Couplers up to 10 cm in length were constructed using the geometry shown in Figure 1(b). Figure 1(c) shows a single frequency coupler which has a parallel input and output. The edge coupler is incorporated into a dispersion compensating geometry in Figure 1(d) which permits the simultaneous excitation of surface plasmons over a broadband of infrared frequencies.

The optical layout for the spectroscopic measurements is shown in Figure 2. A Nerst glower is focussed by an off axis ellipsoidal mirror

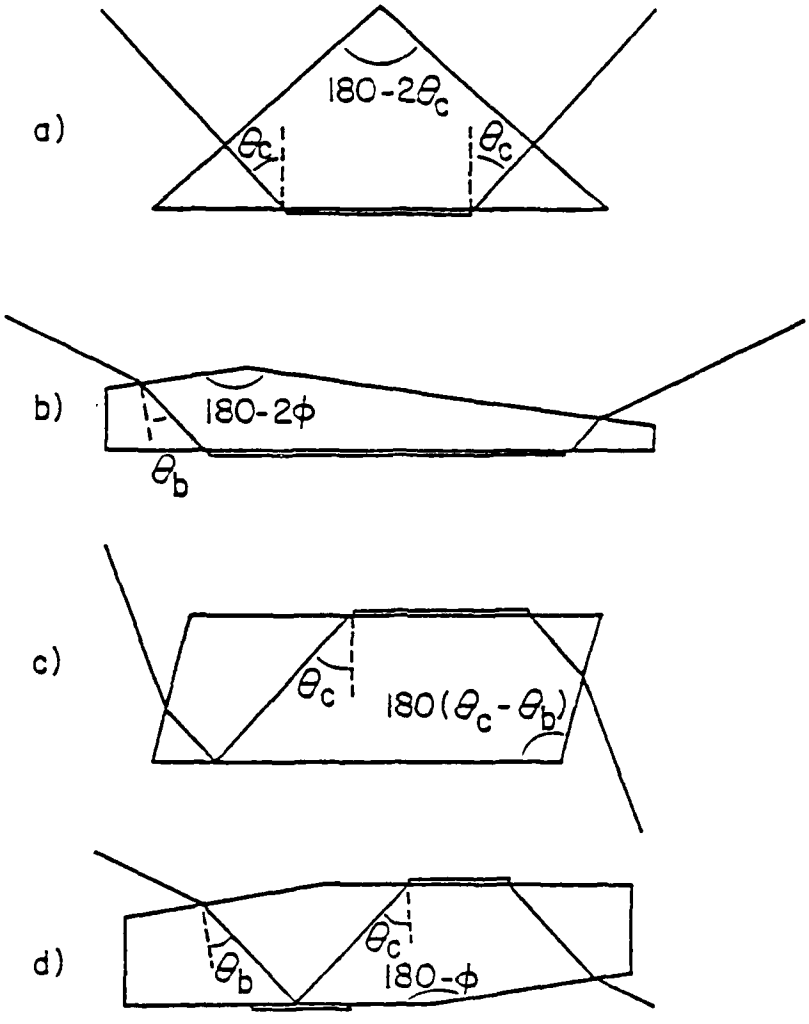

FIGURE 1. Four types of dielectric-metal edge couplers. The metal is represented by the double line. The optical path is shown by the thick solid line. (a) prism coupler, (b) trapizoid coupler, (c) single frequency coupler with parallel input and output and (d) dispersion compensated coupler which is used for broadband experiments.

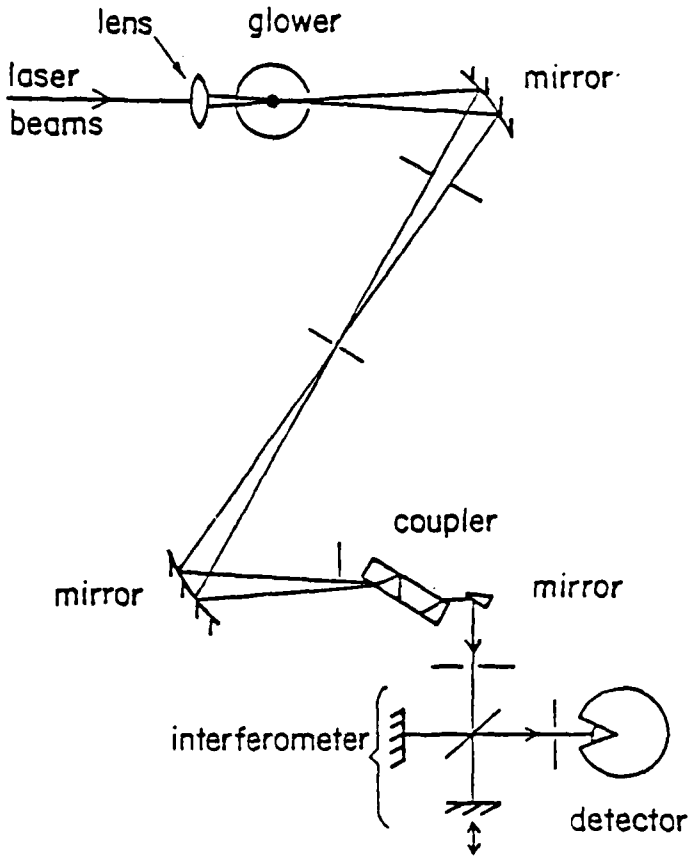

FIGURE 2. Optical layout of the broadband fourier transform SEW spectrometer.

through a pin hole and then off a second ellipsoidal mirror. The point image is focussed on a dispersion compensated KBr coupler. The output from the coupler is deflected by a small mirror to the input of a Michelson interferometer. The output of this interferometer is focussed on an As doped Si photodetector maintained at 4.2° K. A Klinger stepping motor driver is used to advance the interferometer mirror in 2 μ intervals. Because the entire assembly requires precise alignment, a CO_2 laser is first used to align the coupler and interferometer and then the incoherent source is inserted in the optical path as shown in Figure 2.

To explore the sensitivity of the surface plasmon technique, optically thick Au and Ag films were thermally evaporated onto the KBr couplers. Next without breaking the vacuum, a $KReO_4$ overlayer was evaporated over part of the film. The surface plasmon transmission spectrum of a 1.7 cm long gold film covered by approximately one monolayer of $KReO_4$ is shown in Figure 3. The vibrational mode of the ReO_4^- molecule produces the absorption line at 930 cm^{-1}. The four traces show the absorption line at different spectral resolution. Starting from the top of the Figure, the resolution is increased by a factor 2 between each of the spectra. Notice that the bottom two traces look almost the same although the resolution is theoretically increased by a factor 2. The cause of this discrepancy is the Klinger drive mechanism. The translation track makes use of a continuous line of ball bearings. We find that whenever one of these balls approaches or leaves the track the resolution of the instrument is lost. It appears that the ultimate resolution of this interferometer is limited to an optical path which corresponds to the diameter of one ball bearing. Although this resolution is too small to be of much spectroscopic use, it still has been possible to compare the sensitivity of this surface plasmon technique to

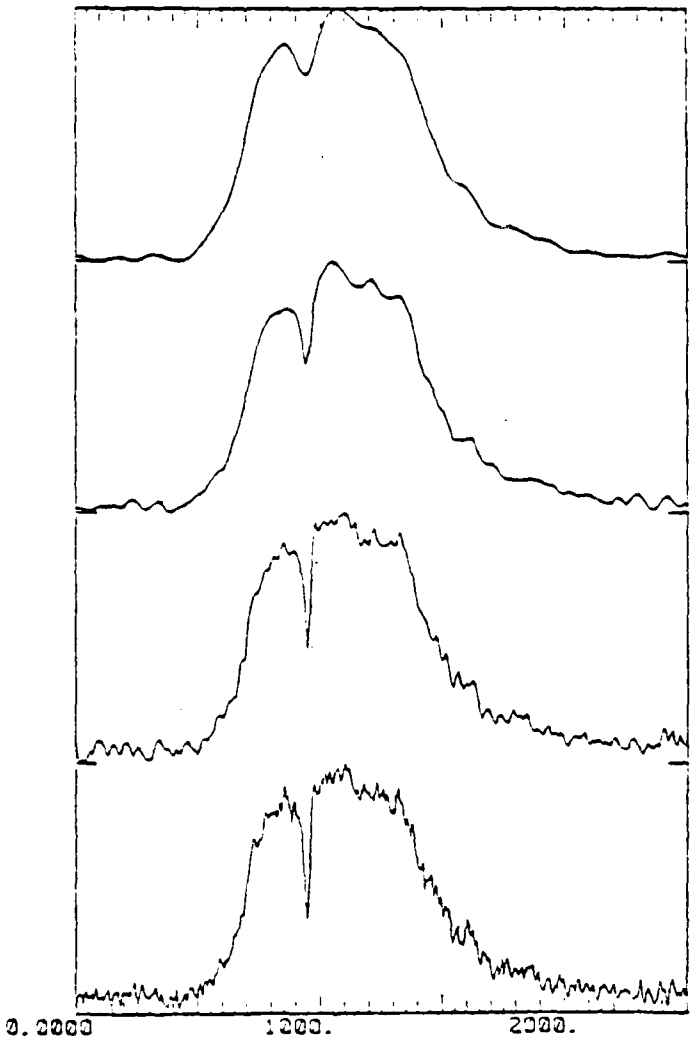

FIGURE 3. Surface plasmon transmission spectrum of one monolayer of $KReO_4$ on Au. The four traces show the unresolved absorption line at four different spectral resolutions. The resolution increases by a factor 2 between each of the spectra.

to that obtained from reflection spectroscopy.

We find that as long as the sample length is adjusted to be approximately equal to the surface plasmon propagation length in the infrared region of interest, then surface plasmon spectroscopy enhances the integrated optical density of an absorption feature by at least an order of magnitude over reflection spectroscopy.

B. Attenuation and Coupling of Far Infrared Surface Plasmons

With the aid of prism and edge coupling techniques surface plasmons have been generated in the mid-infrared part of the spectrum. Measured surface plasmon attenuation coefficients are in reasonable agreement with Drude theory in this region. Efforts by earlier investigators to extend these techniques to longer wavelengths have resulted in anomalously large attenuation coefficients for metal surfaces which were not in agreement with Drude theory.

In publications (B) and (C) we describe our measurements of far infrared surface plasmon transmission on Ge coated Au and Pb surfaces. The surface plasmon attenuation coefficients measured on surfaces with Ge overlayers thicker than about 0.5 μ are found to be in rough agreement with Drude theory. For dielectric thickness smaller than 0.5 μ the attenuation coefficients are anomalous both in their magnitude and thickness dependence. We conclude that bulk electromagnetic waves transmitted along the metal surface account for most of the observed signal in that region. This interpretation is substantiated by a calculation of SEW and bulk wave coupling efficiencies as a function of overlayer thickness. Spreading of the bulk wave packet in the direction perpendicular to the surface as it propagates

along the surface accounts for the large attenuation coefficients previously attributed to surface plasmons on bare metal surfaces.

The reason the inhomogeneous wave coupling technique works well in one frequency region (the IR) but not in another is that the surface plasmon field profile height does not scale with wavelength whereas the evanescent field height of the input coupler does.

Evanescent wave coupling to the bare metal FIR surface plasmon could be enhanced with the addition of a graded dielectric overlayer. The input evanescent beam would couple to a region of the metal with a thick dielectric overlayer, excited surface plasmons would couple to surface plasmons on regions of successively thinner overlayer until bare metal was reached. The addition of a three step dielectric strip on Au as shown in Figure 4 should increase the power ultimately coupled into an 84 cm^{-1} bare surface plasmon by an order of magnitude.

C. p-type InSb-NiSb Eutectic

(1) Spectroscopic Results

To grow the two phase semiconductor crystal, one starts with a eutectic mixture of InSb-NiSb heated above the melting point and then lowers it at constant velocity (e.g., 1 cm/hr) through a steep temperature gradient. Because of this crystal growing technique, the alloy is constrained to undergo a transformation unidirectionally with constant velocity. A transverse section normal to the growth axis reveals a periodic arrangement of NiSb rods in an InSb matrix. The periodic growth is controlled by diffusion. The more uniform the temperature gradient the more perfect the periodic arrays. Our samples contained NiSb fibers 0.5 μ diameter by 20 μ

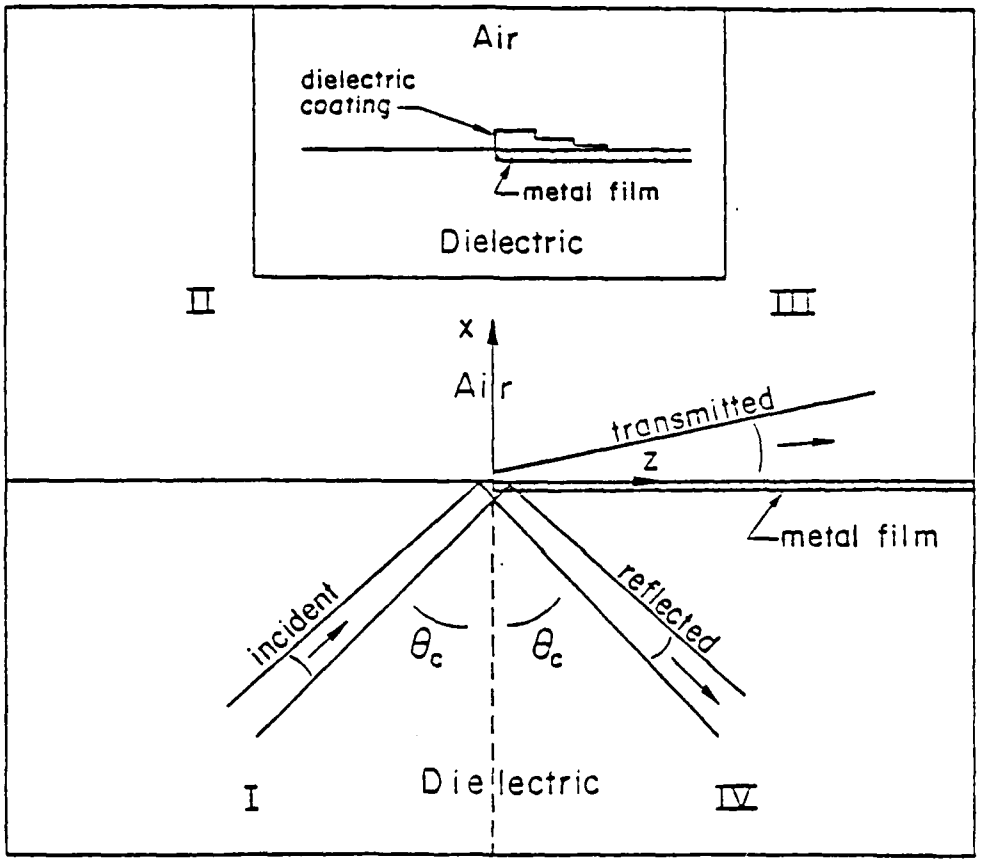

FIGURE 4. The different electromagnetic waves present at a metal edge. The surface plasmons are represented by the arrow in the z direction. The insert shows a graded dielectric overlayer for efficient surface plasmon coupling.

long spaced by about 4 μ in the InSb matrix.

The d.c. electrical properties of the two phase InSb-NiSb eutectic are to a large extent controlled by the parallel aligned metallic NiSb fibers within the semiconducting InSb matrix. Qualitatively, the combination of the two materials in this form results in a medium with highly anisotropic electrical properties. The electrical conductivity is large in the direction of the NiSb fibers and relatively small in the direction orthogonal to the fibers. Also, due to the NiSb fibers, this eutectic displays magneto-resistive properties even more dramatic than those of pure InSb.

Report (D) describes the first comprehensive magneto-optical study of a metal-semiconductor two phase composite medium. Fourier transform transmission spectra below 350 cm^{-1} and the CO_2 laser at 933 cm^{-1} have enabled us to obtain a great deal of energy level information.

By measuring the zero-field far-infrared transmission spectra of the InSb-NiSb eutectic at a variety of temperatures we identified two broad absorption bands which appeared similar to those found in p-type InSb. The temperature-independent band was identified with the eutectic reststrahl while the temperature-dependent absorption was identified with acceptor impurities in p-type InSb. A search for some specific contribution of the NiSb fiber to the zero-field spectrum was made by measuring the spectra of eutectic samples with the NiSb fibers oriented parallel and orthogonal to the k vector of the incident radiation. No difference was observed either because the effect was masked by the large line width of the resonances or because the electric field vector of the radiation was orthogonal to the NiSb fibers in both sample configurations.

A second series of experiments involved the magneto-far-infrared properties of the eutectic. Many field-dependent resonances whose absorption strengths varied with the temperature were observed. The analysis of the eutectic data was based on the observation that the field dependence of two resonances in the eutectic spectra were similar to two resonances in the spectra of p-type InSb. The resonances in p-type InSb involved transitions from the ground state of an acceptor impurity to acceptor levels associated with Landau levels of the valence band. The similarity between the resonances in the eutectic and p-type InSb motivated the calculation of an energy level diagram involving the valence band and acceptor levels of p-type InSb to explain the remaining resonances. The energy level diagram was then successfully tailored for the InSb-NiSb eutectic using the magneto-optical data. This energy level diagram attributes the remaining resonances of the eutectic to intraband transitions and to transitions from acceptor levels to acceptor levels associated with Landau levels of the light-hole valence band.

The field dependence of all the resonances were found to be consistent with this energy scheme for the eutectic.

As with zero-field measurements a search for an anisotropy contribution by the NiSb fibers to the magneto-far-infrared data was made. Again, spectral measurements were made on eutectic samples with the NiSb fibers oriented either parallel or orthogonal to the k vector of the incident radiation. At low temperatures, a small difference was found in the center frequency of the resonances whose frequency position varied with field and a large anisotropic effect was found in a resonance whose center frequency was independent of field. The absorption strength of this resonance decreased with increasing magnetic field for a sample with the NiSb fibers aligned parallel to the

magnetic field. No dependence on field was observed in the strength of the absorption line for a sample with the NiSb fibers aligned orthogonal to the magnetic field.

Several effects due to the interaction of the bound and free holes with the phonons in the eutectic were also observed. The free hole-phonon coupling is apparent in the nonlinear field dependence of the intraband transition while bound hole-phonon coupling is apparent in the field dependence of two resonances whose intial state is the ground state of the acceptor impurity. Both resonances are pinned at approximately the LO phonon frequency. In addition, one of these resonances is pinned at the TO phonon frequency shifted by the ionization energy of the acceptor impurity. Only this last effect has been previously studied in p-type InSb.

Finally, a measurement of the dependence of the energy on the cyrstal momentum (dispersion relation) for the light-hole valence band in InSb-NiSb eutectic was presented. In this measurement, pulsed magnetic fields were employed to shift the frequencies of two intraband resonances through the 10 μ spectral region of CO_2 laser source. The field dependence of these two resonances indicated that the light-hole valence band of the eutectic is more parabolic than the equivalent band in p-type InSb.

In conclusion, the physical properties of InSb-NiSb eutectic have been investigated using far-infrared magneto-optical techniques. By comparison of the eutectic data with experimental data from two previous studies of the p-type InSb, the resonances observed in the eutectic spectra have been identified. These resonances are transitions of the holes among the energy levels of the valence band and acceptor impurity levels. The energy level diagram for the eutectic is similar but not identical to that of p-type InSb. Aside from the shape resonances which we describe below

this difference in band structure is the major effect of the metallic NiSb fibers.

(2) Shape Resonances

Figure 7 in Report (D) shows a set of experimental results which we have been able to identify with shape resonances in the metallic needles. The key experimental results are as follows:

a) A strong resonance is centered at 60 cm^{-1} and a weak resonance centered at 300 cm^{-1}.

b) The resonance strength is anisotropic i.e. the resonance is observed for $\vec{k}_{||}$ fibers and not observed for $\vec{k}_{\perp}$ fibers.

c) The change in strength of the resonance is proportional to the magnetic field squared.

d) The strength of the resonance is independent of temperature as long as the conductivity of the InSb matrix is constant and smaller than ~ 18 $(\Omega\text{-cm})^{-1}$.

To understand these experimental results in detail it is helpful to consider first the problem of an electromagnetic wave incident on a fine wire of infinite length. If the $\vec{k}$ vector of the radiation is perpendicular to the wire axis then there are two cases to consider: either $\vec{E}$ is perpendicular to the wire, or parallel to it. If $\vec{E}$ is perpendicular to the wire then the electrons in the metal have a natural resonance at

$$\omega_{\perp}^2 = \omega_p^2/(1 + \varepsilon_o) \qquad (1)$$

where ω_p is the plasma frequency of the metal and ε_o is the dielectric constant of the host medium.

The measured ε_0 of the InSb composite is 17.6. The plasma frequency of a typical metal is about 5 eV so this particular resonance occurs in the visible part of the spectrum and is not of interest to us.

For the $\vec{E}$ parallel to the wire

$$\omega_{||}^2 = 0$$

the electrons feel no restoring force but the induced current produces a reflected wave with the same polarization. In the limit which we are considering where the wire spacing is much less than the wavelength in the medium the result is a completely reflected wave. For this propagation direction the medium acts like a polarizer.

For $\vec{k}_{||}$ to the wire a surface plasmon mode exists in which the velocity of the wave along the wire is $c/\sqrt{\varepsilon_0}$ but the wave has its maximum amplitude at the wire surface. The dispersion curve for this case is contrasted with that for $k_{\perp}$ rods in Figure (5). The solid line represents the dispersion curve for a wire of infinite length.

Since it is known that the metallic wires in InSb are of finite length, say d, then only standing surface plasmon solutions will be allowed. The condition for a shape resonance is $\frac{n\lambda}{2} = d$ where n = 1, 2,... and λ is the wavelength in the medium. Because these fibers have random spacing in the composite medium only those resonant modes which have a net dipole moment can be excited by a uniform E and M wave. The infrared active excitation wavelengths are

$$\lambda_1 = 2d,\ \lambda_3 = \frac{2d}{3},\ \lambda_5 = \frac{2d}{5},\ldots.$$

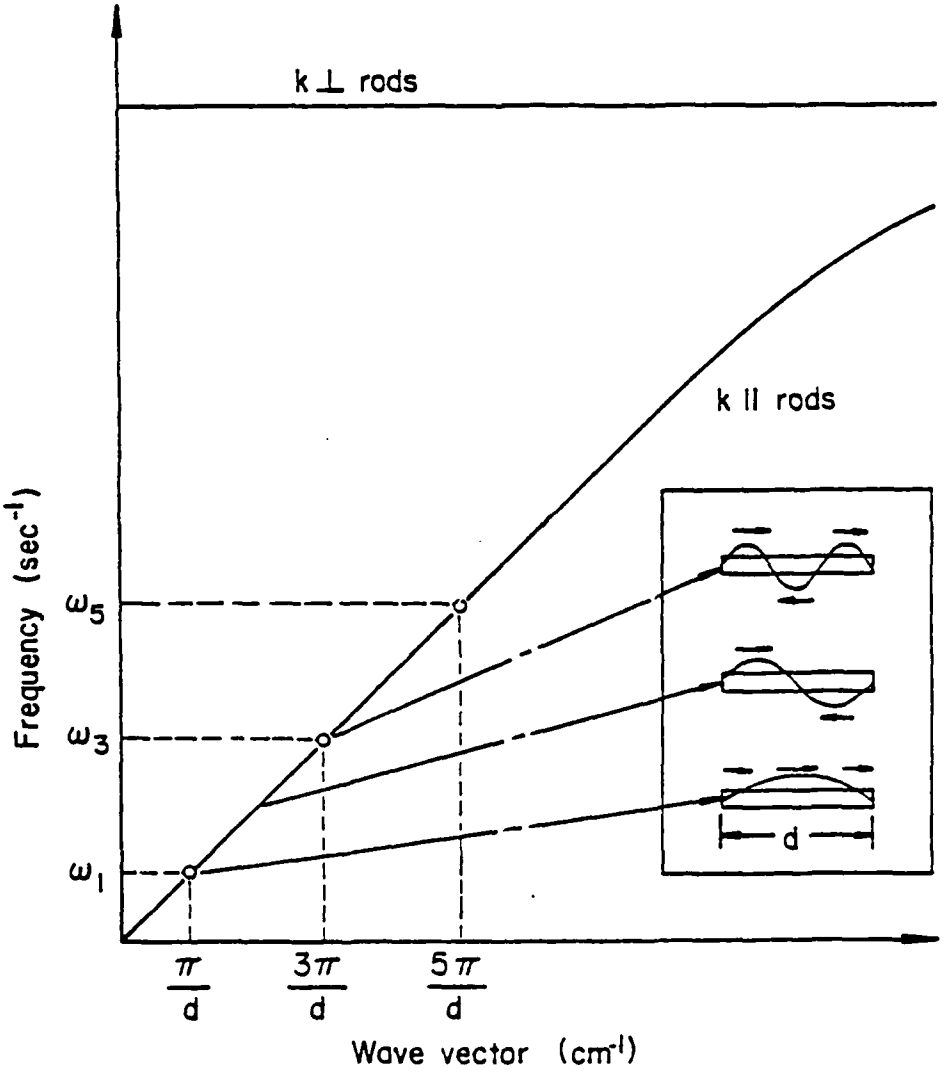

FIGURE 5. Dispersion curve for surface plasmon modes in a thin wire. A optic mode cylinder resonances is excited for k⊥ rod and an acoustic mode surface plasmon is excited for k|| rod. The insert shows the discrete modes allowed when the wire has a finite length, d.

with resonant frequencies

$$\omega_1 = \frac{\pi}{d\sqrt{\varepsilon_o}} \ , \ \omega_3 = \frac{3\pi}{d\sqrt{\varepsilon_o}} \ , \ \omega_5 = \frac{5\pi}{d\sqrt{\varepsilon_o}} \ , \ldots .$$

These normal modes are identified in the insert in Figure 5 . Note that the strength of a given mode is proportional to its net dipole moment squared so the strength should decrease rapidly with increasing harmonic number in the following manner: $1, \frac{1}{9}, \frac{1}{25}, \ldots .$

The experimentally determined resonance at 60 cm^{-1} predicts that $d \tilde{\sim} 20\ \mu$ which is consistent with the values obtained from electron micrographs of eutectic sections. The third harmonic cannot be identified because it is obscured by the reststrahl absorption at 190 cm^{-1}. A resonance is observed at 300 cm^{-1}, the fifth harmonic, which is much weaker than the 60 cm^{-1} resonance.

To account for the magnetic field dependence described, we note first that the absorptivity of a metal in the low frequency limit where $\omega\tau << 1$ can be written as

$$A = \sqrt{\frac{2\omega}{\pi\sigma_o}}$$

where σ_o is the d.c. conductivity of the metal. Since the parallel magneto-resistance of a metal varies as H^2 we take $\sigma(H) = \sigma_o - aH^2$ for NiSb. The magnetic field dependence of the absorptivity simplifies to

$$\frac{A(H) - A(0)}{A(0)} \tilde{=} \frac{1}{2} \frac{aH^2}{\sigma_o}$$

where $\frac{aH^2}{\sigma_o} << 1$.

The shape resonance concept is also consistent with the disappearance of the absorption at 80° K. As temperature is increased from 4.2° K thermal acceptors are created in the InSb. With sufficient concentration these acceptors can short out the oscillating polarization in the rods i.e. the E_z component of the radiation cannot distinguish between the rods and the InSb. How much acceptor conductivity, σ_a, is required to remove the longitudinal polarization P_z in a far infrared period?

$$\frac{dE_z}{dt} = \frac{-4\pi\sigma_a E_z}{\varepsilon_o}$$

so $\tau = \frac{\varepsilon_o}{4\pi\sigma_a} = \frac{1}{\omega}$. We find that $\sigma_a = 18\ (\Omega\text{-cm})^{-1}$, a value which corresponds to that measured at 80° K for p-type InSb.[13]

The shape resonance concept describes all of the experimental data with regard to the far infrared absorption line at 60 cm^{-1}. We conclude that a new kind of energy level structure has been observed in this metal-semiconductor composite whose eigenfrequencies depend on the properties of both of the components.

IV REPORTS AND PUBLICATIONS

(A) "Broadband Surface Electromagnetic Wave Spectroscopy," Z. Schlesinger and A. J. Sievers, Surface Science 102, L29-34 (1981).

(B) "Far Infrared Surface Electromagnetic Wave Propagation Lengths," Z. Schlesinger, B. C. Webb and A. J. Sievers, Bull Am. Phys. Soc. 26, 358-359 (1981).

(C) "Attenuation and Coupling of Far Infrared Surface Plasmons," Z. Schlesinger, B. C. Webb and A. J. Sievers, Solid State Communications 39, 1035-1039 (1981).

(D) "Intraband Magneto-optical Studies of InSb-NiSb Eutectic," A. K. Chin and A. J. Sievers, Jour. Appl. Phys., 52, 7380 (1981).

V PROFESSIONAL PERSONNEL

A. K. Chin	graduate student
Z. Schlesilnger	graduate student
B. C. Webb	graduate student
A. J. Sievers	Professor in charge

END

FILMED

5-86

DTIC